PCCP

Accepted Manuscript

ROYAL SOCIETY OF CHEMISTRY

www.rsc.org/pccp

Synergistic effect of inert oxide and metal fluoride dual coatings on advanced cathode materials for lithium ion battery applications

Kwangjin Park*, Byoung-Sun Lee, Jun-Ho Park, Suk-Gi Hong*

Energy Lab, Samsung Advanced Institute of Technology SAIT, Electronic Materials Research Complex, 130 Samsung-ro, Gyeonggi-do, [16678], Republic of Korea

E-mail: ydmj79.park@samsung.com, bs6002.lee@samsung.com, junho11.park@samsung.com, sukgihong@naver.com

*Corresponding author

Tel.: +82-31-8061-1250

Fax: +82-31-8061-1339

E-mail: ydmj79@gmail.com, sukgihong@naver.com

Postal address: Energy Lab, Samsung Advanced Institute of Technology SAIT, Electronic Materials Research Complex, 130 Samsung-ro, Gyeonggi-do, [16678], Republic of Korea

ABSTRACT

The effect of Al_2O_3/LiF dual coatings on the electrochemical performance of over-lithiated layered oxide (OLO) has been investigated. A uniform coating of Al_2O_3 and LiF is obtained on the surface of the layered pristine material. The OLO with a dual Al_2O_3/LiF coating with a ratio of 1:1.5 exhibits excellent electrochemical performance. An initial discharge capacity of 265.66 $mAh \cdot g^{-1}$ is obtained at a C-rate of 0.1C. This capacity is approximately 15 $mAh \cdot g^{-1}$ higher than that of pristine OLO. The capacity retention (92.8% at the 50^{th} cycle) is also comparable to that of pristine OLO (91.4% at the 50^{th} cycle). Coating the cathode with a dual layer comprising Al_2O_3 and LiF leads to improved charging and discharging kinetics, and prevents direct contact between the cathode and the electrolyte.

Keywords: Over-lithiated layered oxide, LiF, Al_2O_3

1. Introduction

The worldwide market for battery-powered electric vehicles (EVs) has grown rapidly, necessitating the development of high-energy-density batteries for the mass storage of electricity. Li-ion rechargeable batteries (LIBs) have attracted significant attention as promising energy and power storage systems for future EV sowing to their high energy densities and long cycle life.[1–4] However, conventional cathode materials for LIBs such as $LiCoO_2$ and $LiMnO_2$ are unable to deliver the high energy densities required from the high power LIBs for powering EVs and hybrid electric vehicles (HEVs) because of their limited capacity. Therefore, the recent development of over-lithiated layered oxides (OLOs), $x Li_2MnO_3 \cdot (1-x)\ Li\boldsymbol{M}O_2$, ($\boldsymbol{M}$ = Co, Mn, Ni) with exceptionally high reversible capacities (> 250 $mAh \cdot g^{-1}$) as cathode materials for LIBs has drawn much attention.[3,5,6] Although Li-rich layered oxides have numerous advantages, they have insufficient structural stability during cycling owing to the presence of complex lattice units consisting of the Li_2MnO_3 and $Li\boldsymbol{M}O_2$ phases that are formed in the initial crystal structures of OLOs.

In order to overcome these demerits of Li-rich layered oxides and further enhance the electrochemical performance of the LIBs, surface modification of the cathode material (e.g., by applying a surface coating) is conventionally adopted and is known to be

effective.[5,7–13] Inert materials such as Al_2O_3 and ZrO_2 are generally coated on the surface of the cathode in order to suppress the reaction between the cathode and the electrolyte. However, these materials lead to loss of capacity and lower the rate performance because of the poor electronic conductivity of the coated material.[5,7,8,13] Therefore, other materials such as aluminum fluoride (AlF_3) have been selected as the coating material for enhancing the electrochemical performance of the cathode. Additionally, other metal fluorides such as CaF_2 and CeF_2 have also been coated on the OLOs.[10,12] Li et al. confirmed that coating the cathode with a metal fluoride led to enhanced cycle performance.[11] It has been previously reported that coating with fluoride materials assists in phase transformation from the layered structure.[9–11] So far, most of the studies on cathode coatings have focused on a single coating material.

Herein, we examine the synergistic effect of a combination of coating materials consisting of inert oxide and fluoride. In particular, the combination of LiF and Al_2O_3has been studied. The coating quality has been investigated by transmission electron microscopy (TEM), scanning electron microscopy (SEM), and X-ray photoelectron spectroscopy (XPS) analyses and the electrochemical performance of the dual coatings has been systematically characterized by electrochemical measurements using 2032 coin cells.

2. Experimental

2.1. Sample preparation

OLO was synthesized by a co-precipitation procedure. Appropriate amounts of Ni, Mn, and Coprecursors (Ni/Co/Mn=25:10:65) were dissolved in de-ionized (DI) water and stirred to obtain a homogeneous solution. Next, the chelating agent (NH_4OH) and a stoichiometric amount of NaOH solution were added to allow co-precipitation after sufficient stirring. The co-precipitated $(NiMnCo)(OH)_2$ was co-ground with a stoichiometric amount of Li_2CO_3 and the ground material was calcined at 900°C. Next, aluminum nitrate nonahydrate was dissolved in ethanol, whereas ammonium fluoride was dissolved in a mixture of ethanol and DI water. The OLO powder was then immersed in the aluminum nitrate nonahydrate solution, following which the ammonium fluoride solution was slowly added to the mixture with a dropper. The resulting solution was stirred continuously at 80°C until the solvent completely evaporated. The resulting coated OLO sample was heated at 400°C for 5 h in flowing N_2 gas.

XPS analyses were performed with a Φ Physical Electronics Quantum 2000 Scanning ESCA Microprobe spectrometer using focused monochromatized Al Kα radiation at 1486.6 eV. To avoid external contamination and oxidation, all the samples were

transferred under an inert gas atmosphere from the glove box to the analysis equipment using a specialized transfer vessel. The morphological changes of the OLOs for different surface modification conditions were determined using SEM (Hitachi S-4700N). In addition, HRTEM images were obtained by the FEI Titan Cubed 60-300 microscope equipped with Cs correctors and a monochromator at the acceleration voltage of 300 V. The sample was deposited on a Cu grid covered by a holey carbon film. In addition, energy dispersive spectroscopy (EDS) and electron-filtered TEM (EFTEM) were performed for element mapping of the samples to observe their compositional distributions.

2.2. Electrochemical measurements

The composite positive electrode containing 92wt. % active material, 4 wt. % Denka black, and 4 wt. % polyvinylidenedifluoride (PVDF) was pasted on an aluminum foil, which was used as a current collector. The electrodes were dried at 120°C in vacuum and roll pressed. Metallic lithium was used as the counter electrode. The electrolyte solution was composed of 1.3 $molL^{-1}$ of $LiPF_6$ dissolved in a mixture of fluoroethylene carbonate and dimethylene carbonate. R2032-type coin cells were assembled in a dry room and the cells were discharged and charged galvanostatically. Test per each

condition was conducted using three samples. The loading level was 1 mAh/cm^2. Further, the electrochemical activities of the cathodes were characterized by electrochemical impedance spectroscopy (EIS) using a Solartron 1260 frequency-response analyzer. The impedance measurements were conducted over an applied frequency range of 10 mHz to 1 MHz. The EIS measurements were performed on the cells in the charged and discharged states during cycling.

3. Results and Discussion

XPS analysis was performed to directly confirm the chemical states on the surface of the coating layer and the results are shown in Figure 1. In the Al 2p core level spectrum, the XPS peak at 73.9 eV corresponds to $Al(OH)_2$ and Al_2O_3,whereas the small shoulder peak at ~75.2 eV indicates the presence of the Al-O-F_x chemical state. The XPS spectra of the Al 2p core level allow accurate characterization of Al_2O_3 and Al-O-F_x under various surface modification conditions. The prevalence of Al_2O_3 chemical is detected in samples that were coated using Al_2O_3. Although the cathode material was coated with Al_2O_3 and LiF, AlF_3 was barely detected.[14] A similar tendency is observed in the F 1s core level structure, in which the peaks correspond to the LiF state.

Figure 2 (a)-(d) show SEM images obtained for the pristine OLO samples as well as for the Al_2O_3, LiF, and Al_2O_3/LiF coated OLO samples. The surface morphology did not greatly change for different coating types. Additionally, the coating layer was confirmed to be uniform from the TEM images of the cathode surface shown in Figure 2 (e)-(f). Figure 2 (f) displayed the selected area electron diffraction (SAED) pattern for regions marked 1 in (f). The SAED pattern exhibited layered structure.[15] The satellite spot of different phase by coating material was hard to recognize. That might be due to too small amount of coating material compared to OLO and low crystallinity of coating material. To confirm the composition of the coating layers over the surface of OLO, the EDS and EF-TEM analysis were performed, which was shown in Figure 2 (g)-(h). The concentration of Al is especially high at the surface of the powder. The distribution of F is confirmed to be located outside the F through EFTEM (Figure 2 (h)). Although the cathode was coated with two materials, the two materials did not appear as separate layers and a single uniform coating was observed.

Figure 3(a) shows the potential versus capacity profiles of OLO and surface modified OLOs during the 1st cycle at 0.1C.At a cutoff voltage of 2.5 V, the cells containing pristine OLO, Al_2O_3, LiF, Al_2O_3/LiF modified cathodes delivered reversible capacities of ~251.3 mAh·g^{-1}, ~236.7 mAh·g^{-1}, ~254.2 mAh·g^{-1}, and ~255.7 mAh·g^{-1},

respectively. The Al_2O_3 modified sample exhibited the lowest capacity, since surface modification with inert Al_2O_3 caused an increase in the charge transfer resistance. Generally, the capacity is decreased after coating due to the formation of resistive layer by coating. On the other hand, the capacities of the LiF-modified and Al_2O_3/LiF modified samples were higher than that of the pristine sample, which may be due to enhanced kinetics owing to improved electronic conductivity. Previous studies have reported that coating with fluoride materials leads to phase change from Li_2MnO_3 to the spinel-like phase, which has a higher electronic conductivity than Li_2MnO_3. The higher electronic conductivity imparted by the fluoride material leads to enhanced electrochemical performance.[10–12] In the case of the Al_2O_3/LiF modified sample, although Al_2O_3 exists in the coating layer, the capacity did not decrease, which might be from the uniform mixing of Al_2O_3 and LiF, as shown in Figure 2 (g).

Figure 3 (b) compares the cycling performance of the cells at 25 °C at a constant rate of 1C. The capacity retention values were 91.4%, 94.9%, 89.4%, and 92.2% at the 50th cycle for the pristine OLO, Al_2O_3, LiF, and Al_2O_3/LiF modified samples, respectively. All the surface modified samples exhibited higher capacity retention compared to the pristine sample. In particular, the capacity retention of the Al_2O_3 modified sample was remarkably high since the reaction between the electrolyte and the cathode was blocked

at high charging voltage, as reported previously.[5,7,8] In particular, the charge voltage of OLO was higher than that of other typical cathode materials, which allowed a high capacity. At a high charging voltage of 4.6V, chemical safety is a key factor that must be considered for achieving stable cycle performance. LiF coating sample showed the capacity drop after 45 cycles. LiF, which was one material of SEI layer, was continuously formed on the cathode surface during the cycle caused by decomposition of electrolyte and reaction with electrolyte and cathode at high charging voltage.[16] For LiF coated sample, the thicker LiF compared to other samples might lead to sharper capacity drop after 40 cycle because the LiF was very low ionic conductivity.[16] By preventing the reaction between the cathode and the electrolyte by acting as a barrier, the Al_2O_3 coating leads to enhanced cycle performance.

The capacity retention of the Al_2O_3/LiF modified sample was also improved, although the extent of improvement was different compared to case of the Al_2O_3-only coating. The LiF/Al_2O_3 modified sample exhibited higher electrochemical performance and cycle retention, owing to synergistic effect between the two materials.

EIS measurements were next conducted to investigate the differences in the electrochemical polarization effects between the samples. The impedance of a two-electrode coin cell was measured after the first charge/discharge cycle. The EIS spectra

(Nyquist plots) and the equivalent circuit used to fit these spectra are presented in Figure 4 (a) and (b). The measured EIS spectra can be considered in three parts in relation to the charge/discharge process. The DC resistance (R_s in the equivalent circuit) mainly arises from the resistance of the electrolyte. The impedance in the intermediate-frequency region, i.e., charge transfer resistance (R_{ct}), is related to the charge transfer at the cathode–electrolyte interface. On the other hand, the impedance in the low-frequency region, i.e., diffusion resistance (R_{diff}), is attributed to both the migration of Li^+ ions through the SEI film and the diffusion of Li^+ in the electrolyte, a phenomenon referred to as Warburg impedance.[17–20]

As evident from the figure, the impedance spectra for all the samples appeared as a single semicircle, i.e., two semicircles were merged into one semicircle. Most of the impedance of the semicircle could be modeled by R_{ct}, owing to the low electronic conductivity of OLO.[21] The pristine material showed the lowest impedance for initial state. The impedance for initial state as shown in Figure 4 (a) was measured before formation process of coin cell. The impedance might be affected by percolation of electrolyte into cathode and the resistive layer, caused by coating. That led to large impedance for coated samples. However, after the 30th charge/discharge cycle, the radii of the first semicircle decreased for all the samples, as shown in Figure 4 (a) and (b).

This is attributed to the activation of OLO during cycling since the electrolyte diffuses into the cathode during cycling. The lower resistance value arises from the enhanced contact area between the electrolyte and the cathode as well as the stabilized layer on the cathode material.[22] After 30 cycles, significant differences were observed in the impedance values among the samples. The calculated electrochemical impedance parameters were presented in Table 1. For example, the impedance of the LiF surface modified sample was lower than that of the pristine sample, which might be due to the increase in the electronic conductivity caused by phase change during cycling. Among the F-modified samples, the Al_2O_3/LiF dual coated sample exhibited a lower impedance than the LiF coated sample after cycling, which might be due to the more stable SEI layer in the former case.[22] On the other hand, the Al_2O_3 surface modified sample exhibited larger resistance owing to the inert coating layer. The impedance results were consistent with the electrochemical performance.

Next, the influence of the coating process on the morphology of the resulting coating layer was investigated. One-step and two-step coating processes were individually considered. In the one-step coating process, a single coating layer was formed by simultaneously using Al_2O_3 and LiF, whereas in the two-step coating process, the LiF coating was formed first, following which Al_2O_3 was coated on the LiF layer. Figure 5

illustrates the effect of the coating process change on the electrochemical performance of the cathodes. As stated previously, the Al_2O_3coating suppresses the reaction between the cathode and the electrolyte, although it leads to lowered capacity. On the other hand, coating with fluoride materials leads to transformation from Li_2MnO_3 to a spinel-like phase, which exhibits higher electronic conductivity than Li_2MnO_3.[10–12] Owing to the separation of the coating layers in the two-step coating process, the synergistic effect of Al_2O_3 and LiF on the electrochemical performance improvement is expected. Surprisingly, the electrochemical performance of the sample obtained by the two-step process was poorer than that of the pristine sample, suggesting that the advantages of the LiF coating were nullified owing to the presence of the inert Al_2O_3coating. However, the coating layer formed using a homogeneous mixture of Al_2O_3 and LiF exhibited synergistic effect.

The Al_2O_3/LiF ratio was altered sequentially, in order to determine the optimum mixture composition at which the mixing effect of the two materials is maximized. Figure 6 shows the electrochemical performance of samples coated with various compositions of Al_2O_3 and LiF with a fixed total coating weight of 1 wt.%. At a cutoff voltage of 2.5 V, the cells containing pristine and dual coated OLO cathodes with Al_2O_3/LiF ratios of 1:1.5, 1:3, and 1:6 delivered reversible capacities of ~251.3

$mAh \cdot g^{-1}$, ~265.66 $mAh \cdot g^{-1}$, ~255.67 $mAh \cdot g^{-1}$, and ~242.42 $mAh \cdot g^{-1}$, respectively. In other words, the best battery performance was achieved for the sample with an Al_2O_3/LiF ratio of 1:1.5. Although the Al_2O_3-only coated sample led to decreased capacity because Al_2O_3 is an inert material, increase in the amount of Al_2O_3 in the Al_2O_3/LiF dual coating led to improved electrochemical performance. On the other hand, when the amount of LiF was high, the capacity decreased probably due to decline in the amount of Li caused by the excess formation of LiF during phase change from Li_2MnO_3 to the spinel-like phase.[11,12] Moreover, the initial coulombic efficiency increased from 88.4% to 94.4% with increase in the F content due to decrease in the irreversible capacity by $LiMnO_3$. Transformation to the spinel-like phase was indirectly confirmed by the voltage plateau at ~2.8 V, which is characteristic of the $LiMn_2O_4$ spinel structure. This is definitively confirmed in the dQ/dV graph shown in Figure S1.[23-24]

Figure 6(b) compares the cycling performance of the cells measured at 25°C at a constant rate of 1C. The capacity retention values were 92.2%, 92.8%, 92.2%, and 88.1% at the 50th cycle for the pristine sample and dual coated OLO samples with Al_2O_3/LiF ratios of 1:1.5, 1:3, and 1:6, respectively. The capacities of the samples during cycling were similar to the initial capacity. Further, all the surface-modified

cathodes exhibited higher capacity retention during cycling compared to the pristine cathode. For a fixed total coating weight, OLOs with higher Al_2O_3 content exhibited superior cycle retention due to suppression of the reaction between the electrolyte and the cathode at high charging voltage. Similar to tendency of Figure (3), the large amount of F coating showed capacity drop after 45 cycles.

When Al_2O_3 and LiF were simultaneously coated on the cathode material from mixtures of different compositions, smaller LiF and higher Al_2O_3 contents at a fixed coating weight led to enhanced electrochemical performance; this was due to the small degree of phase transformation and lack of contact between the cathode and the electrolyte.

4. Conclusions

The effect of uniform dual coating on OLO on the electrochemical performance was studied. Coating with LiF enhanced the electrochemical performance, whereas Al_2O_3 improved the chemical stability at high charging voltage. Owing to the synergistic effect of the coating layers containing LiF and Al_2O_3, the electrochemical performance and cycle performance of the cells were improved. For OLO samples with a 1:1.5 Al_2O_3/LiF ratio, an initial discharge capacity of 265.66 $mAh \cdot g^{-1}$ was obtained at a C-rate of 0.1C.

This capacity is approximately 15 $mAh \cdot g^{-1}$ higher than that of pristine OLO. Capacity retention of the coated sample (92.8% at the 50^{th} cycle) was also comparable to that of pristine OLO (91.4% at the 50^{th}cycle).

Acknowledgments

References

1 J. Yang, F. Cheng, X. Zhang, H. Gao, Z. Tao and J. Chen, *J. Mater. Chem. A*, 2014, **2**, 1636–1640.

2 C. Liu, F. Li, L.-P. Ma and H.-M. Cheng, *Adv. Mater.*, 2010, **22**, E28–E62.

3 N. Yabuuchi, K. Yoshii, S.-T. Myung, I. Nakai and S. Komaba, *J. Am. Chem. Soc.*, 2011, **133**, 4404–4419.

4 X. Wei, S. Zhang, Z. Du, P. Yang, J. Wang and Y. Ren, *Electrochim. Acta*, 2013, **107**, 549–554.

5 G. Kobayashi, Y. Irii, F. Matsumoto, A. Ito, Y. Ohsawa, S. Yamamoto, Y. Cui, J.-Y. Son and Y. Sato, *J. Power Sources*, 2016, **303**, 250–256.

6 J. Lin, D. Mu, Y. Jin, B. Wu, Y. Ma and F. Wu, *J. Power Sources*, 2013, **230**, 76–80.

7 Y. Kim, H. S. Kim and S. W. Martin, *Electrochim. Acta*, 2006, **52**, 1316–1322.

8 H. Kobayashi, T. Okumura, M. Shikano, K. Takada, Y. Arachi and H. Nitani, *Solid State Ionics*, 2014, **262**, 43–48.

9 Y.-K. Sun, M.-J. Lee, C. S. Yoon, J. Hassoun, K. Amine and B. Scrosati, *Adv. Mater.*, 2012, **24**, 1192–1196.

10 X. Liu, J. Liu, T. Huang and A. Yu, *Electrochim. Acta*, 2013, **109**, 52–58.

11 L. Li, Y. L. Chang, H. Xia, B. H. Song, J. R. Yang, K. S. Lee and L. Lu, *Solid State Ionics*, 2014, **264**, 36–44.

12 C. Lu, H. Wu, Y. Zhang, H. Liu, B. Chen, N. Wu and S. Wang, *J. Power Sources*, 2014, **267**, 682–691.

13 J. Zhao, G. Qu, J. C. Flake and Y. Wang, *Chem. Commun.*, 2012, **48**, 8108-8110.

14 AlainTressaud, *Functionalized Inorganic Fluorides: Synthesis, Characterization and Properties of Nanostructured Solids*, Wiley, 2010, 575-579 .

15 L. Wu, K. Nam, X. Wang, Y. Zhou, J. Zheng, X. Yang and Y. Zhu, *Chem. Mater.*, 2011, 3953–3960.

16 V. A. Online, X. Xiong, D. Ding, Y. Bu, Z. Wang, B. Huang, H. Guo and X. Li, *J. Mater. Chem. A*, 2014, **2**, 11691–11696.

17 K. Karthikeyan, S. Amaresh, G. W. Lee, V. Aravindan, H. Kim, K. S. Kang, W. S. Kim and Y. S. Lee, *Electrochim. Acta*, 2012, **68**, 246–253.

18 S. Kandhasamy, P. Singh, S. Thurgate, M. Ionescu, D. Appadoo and M. Minakshi, *Electrochim. Acta*, 2012, **82**, 302–308.

19 N. Yabuuchi and T. Ohzuku, *J. Power Sources*, 2003, **119-121**, 171–174.

20 K. Karthikeyan, S. Amaresh, V. Aravindan, W. S. Kim, K. W. Nam, X. Q. Yang and Y. S. Lee, *J. Power Sources*, 2013, **232**, 240–245.

21 Y. Fu, H. Jiang, Y. Hu, Y. Dai, L. Zhang and C. Li, *Ind. Eng. Chem.*, 2015, **54**, 3800–3805.

22 K. Park, D. Han, H. Kim, W. Chang, B. Choi, B. Anass and S. Lee, *RSC Adv.*, 2014, **4**, 22798–22802.

23 H. Jiang, Y. Fu, Y. Hu, C. Yan, L. Zhang and P. S. Lee, *Small*, 2014, **10**, 1096–1100.

24 Y. Fu, H. Jiang, Y. Hu, Y. Dai, L. Zhang and C. Li, *ACS Nano*, 2016, **10**, 1648–1654.

Figure captions

Figure 1. XPS core peaks of pristine, Al_2O_3, LiF, and Al_2O_3/LiF-coated OLO cathodes: (a) Al 2*p*, (b) F 1*s*

Figure 2. SEM images of OLO (a) pristine (b) Al_2O_3 coated OLO (c) LiF coated OLO (d) Al_2O_3 and LiF coated OLO and TEM images of (e) pristine (f) Al_2O_3/LiF-coated OLO (g) EDS element mapping images of Al_2O_3/LiF-coated OLO (h) EFTEM image of Al_2O_3/LiF-coated OLO with an image showing F

Figure 3. (a) Comparison of the first charge/discharge characteristics of pristine, Al_2O_3, LiF, and Al_2O_3/LiF coated OLO samples; (b) cycling performances of pristine, Al_2O_3, LiF, and Al_2O_3/LiF coated OLO samples

Figure 4. EIS spectra of pristine, Al_2O_3, LiF, and Al_2O_3/LiF coated OLO samples at the (a) initial state and (b) after 30 cycles

Figure 5.(a) Illustration of cathode material coated using a one-step coating process and a two-step coating process (b) Cycling performances of pristine sample, OLO sample coated with a one-step coating process, and OLO sample coated with a two-step coating

process; (c) relative rate capabilities of pristine sample, OLO sample coated with the one-step coating process, and OLO sample coated with the two-step coating process

Figure 6. (a) Comparison of the first charge-discharge characteristics of pristine and dual coated OLO samples with Al_2O_3/LiF ratios of 1:1.5, 1:3, and 1:6; (b) Cycling performances of pristine and dual coated OLO samples with Al_2O_3/LiF ratios of 1:1.5, 1:3, and 1:6

Table captions

Table 1. The fitted impedance parameters in the equivalent circuit model in Figure 4.

Sample		$R_s(\Omega)$	$R_{ct}(\Omega)$
Pristine	Initial	2.76	60.3
	30^{th} cycle	3.91	22.75
Al_2O_3 coating	Initial	2.72	68.1
	30^{th} cycle	4.45	25.71
LiF coating	Initial	2.51	66.7
	30^{th} cycle	4.81	16.19
Al_2O_3/LiF coating	Initial	2.61	62.5
	30^{th} cycle	3.83	14.86

Figure 1

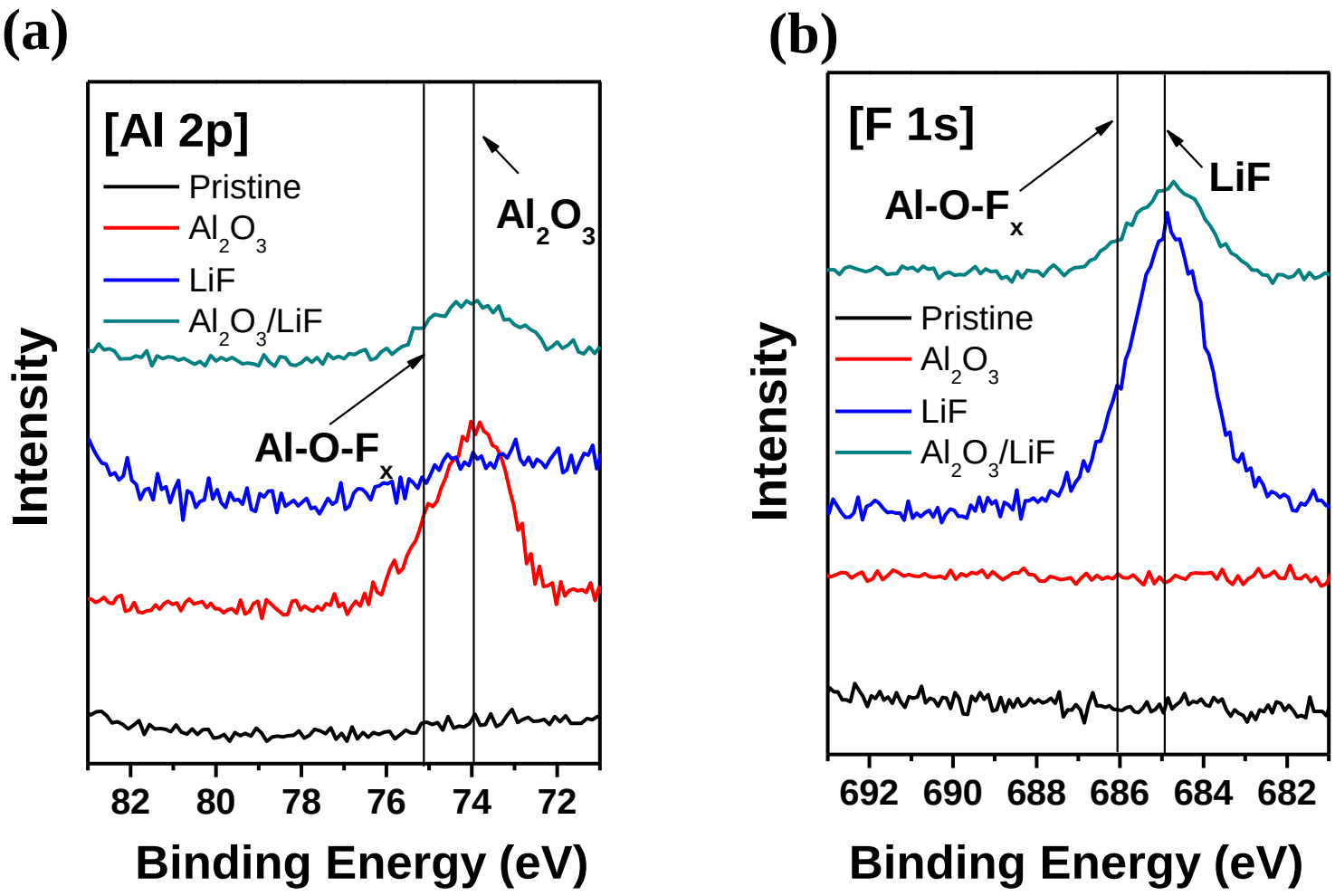

Figure 2

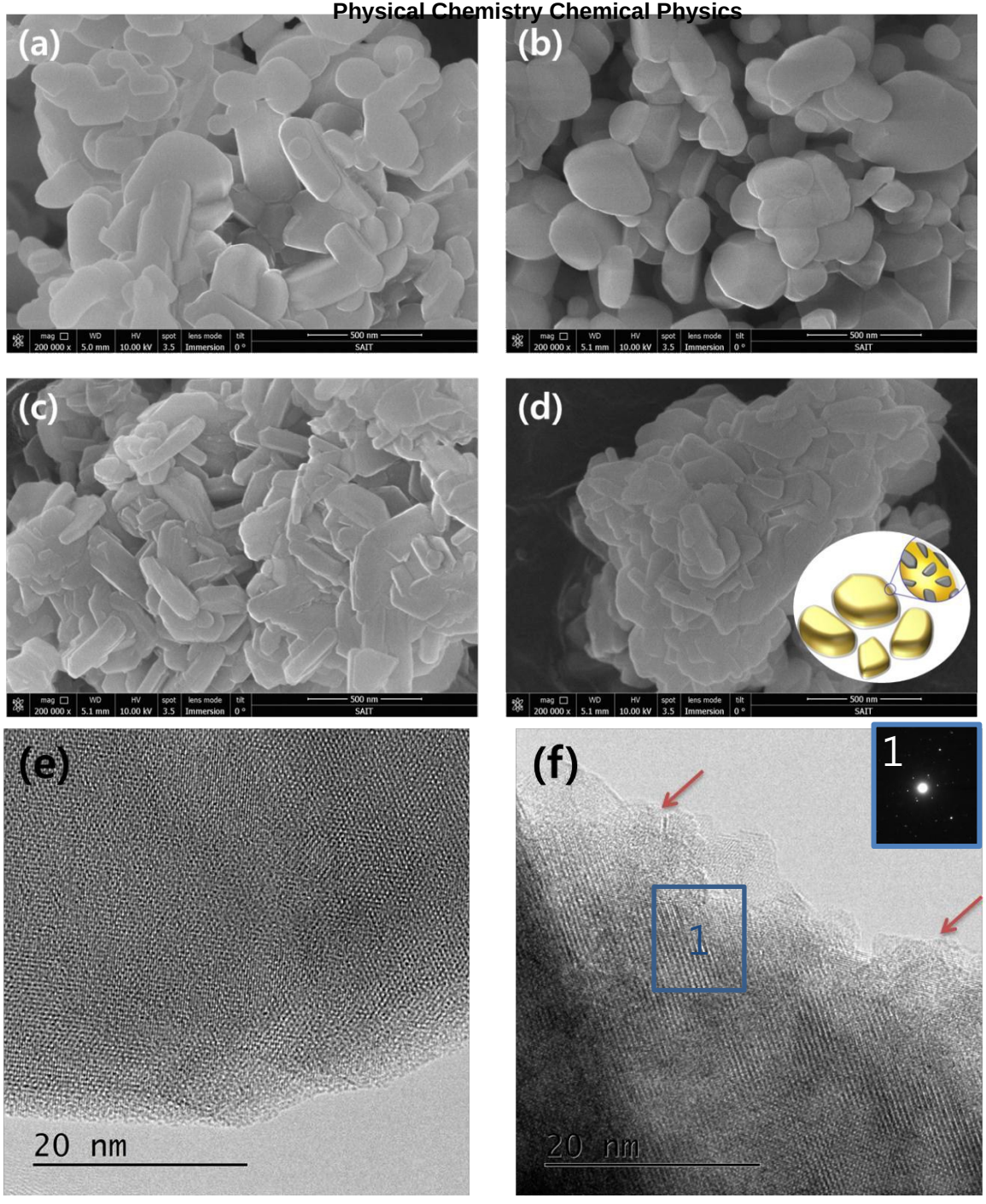

Figure 2

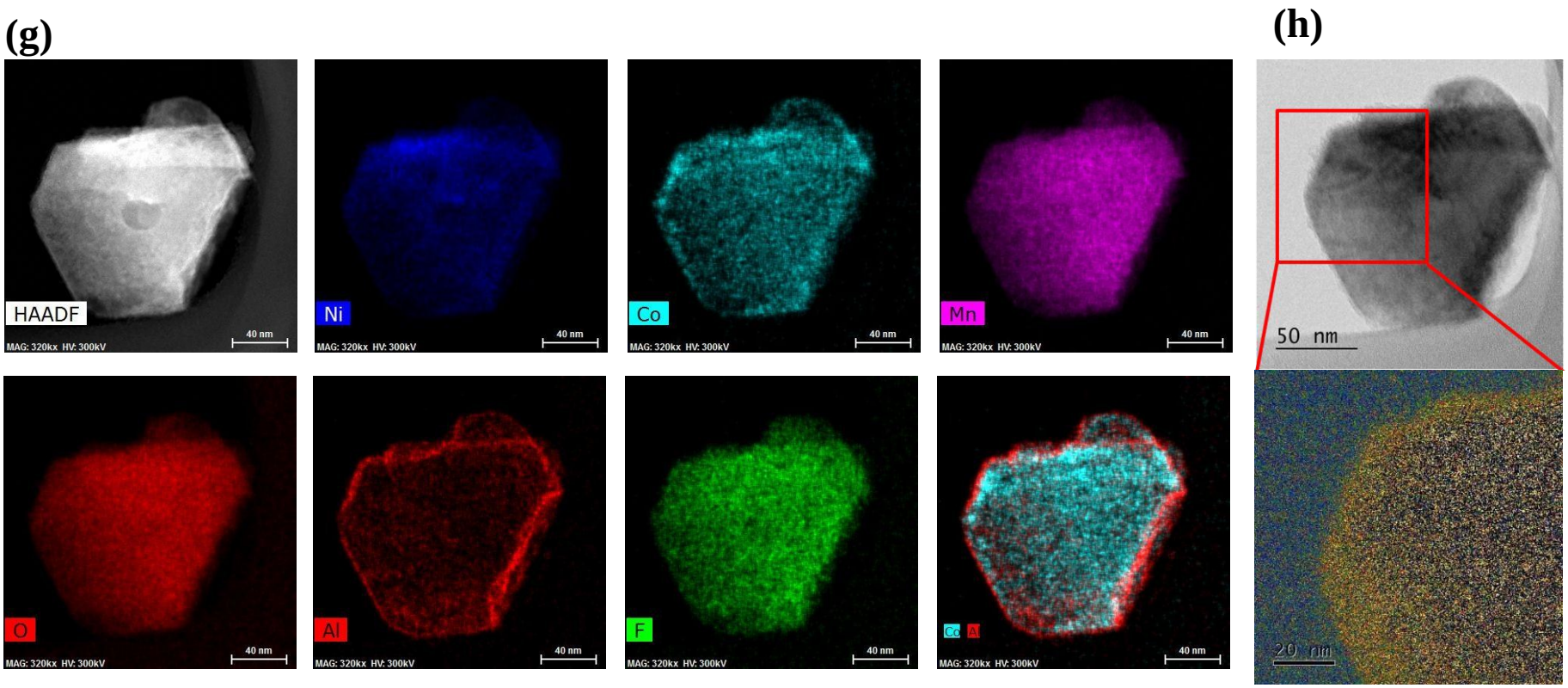

Figure 3

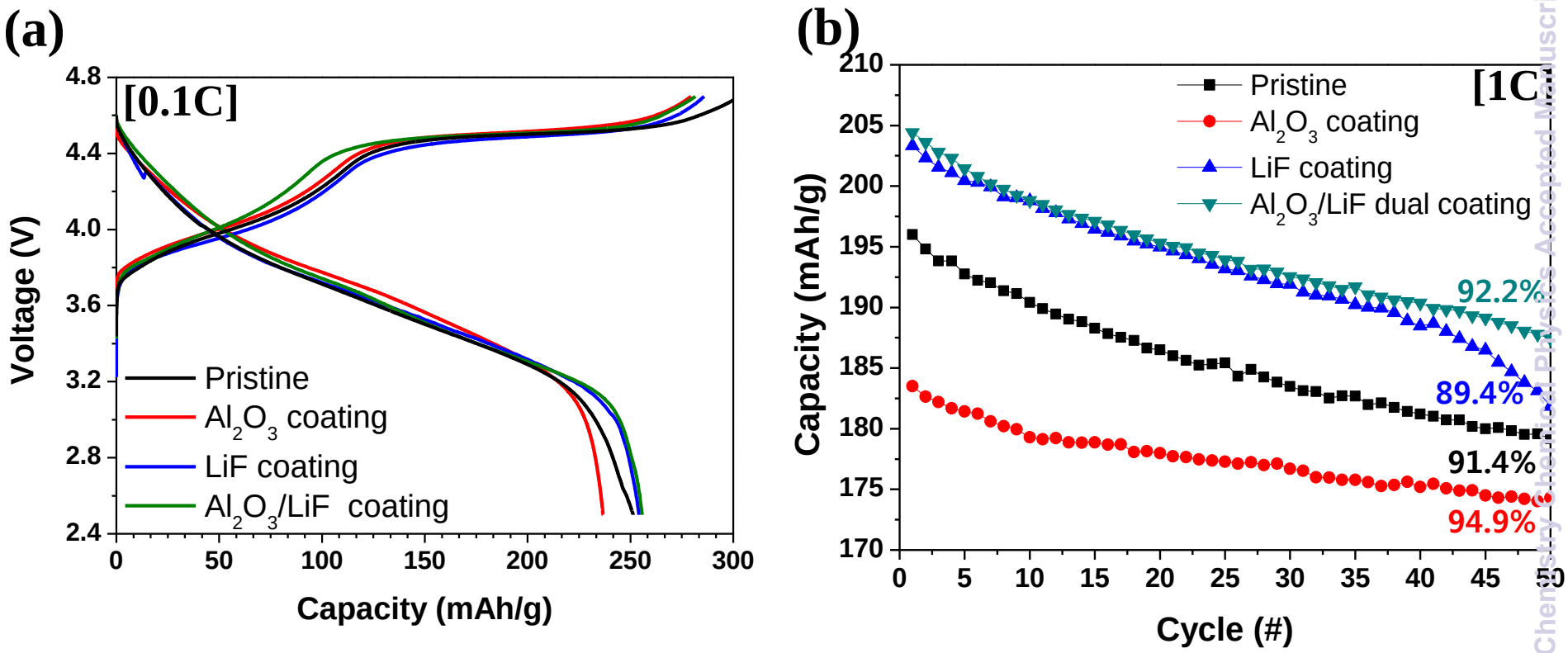

Figure 4

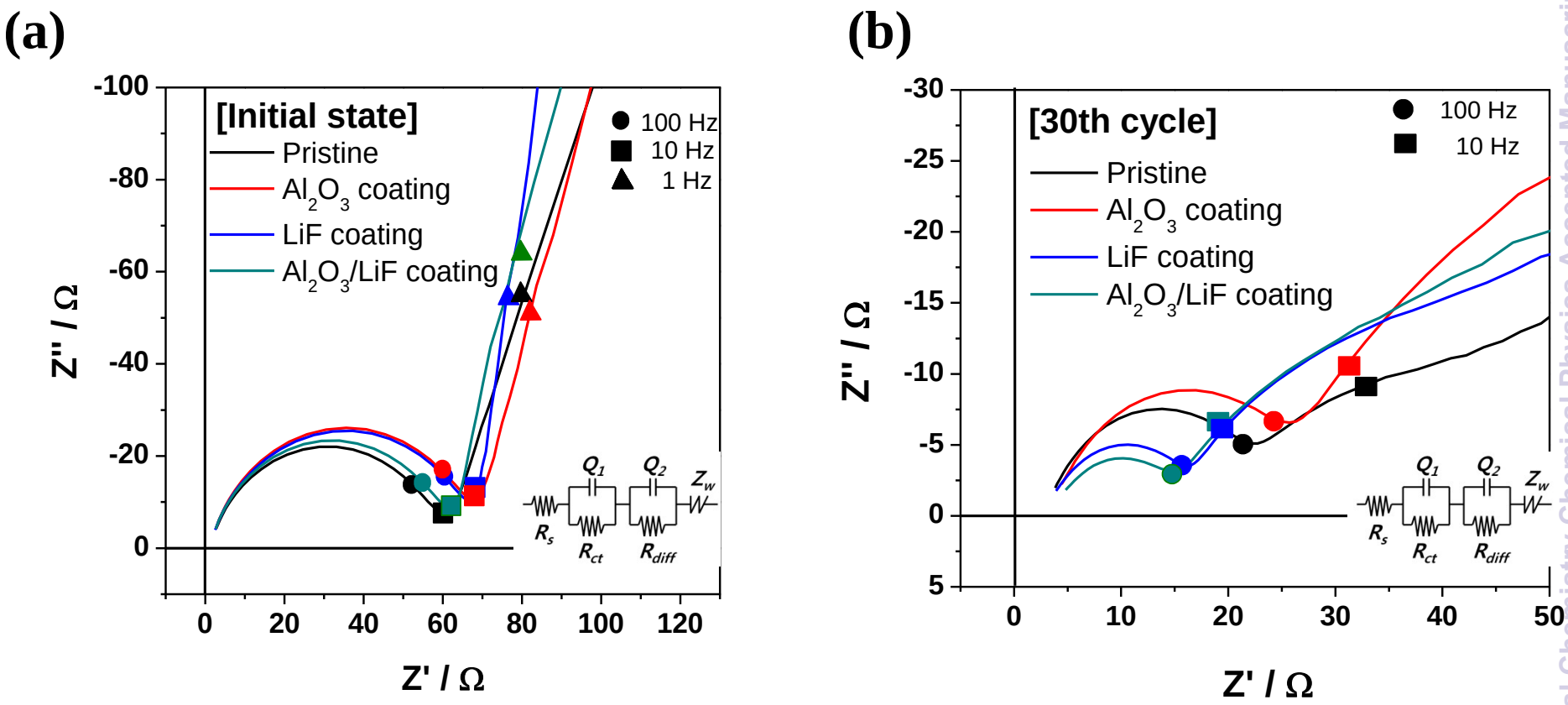

Figure 5

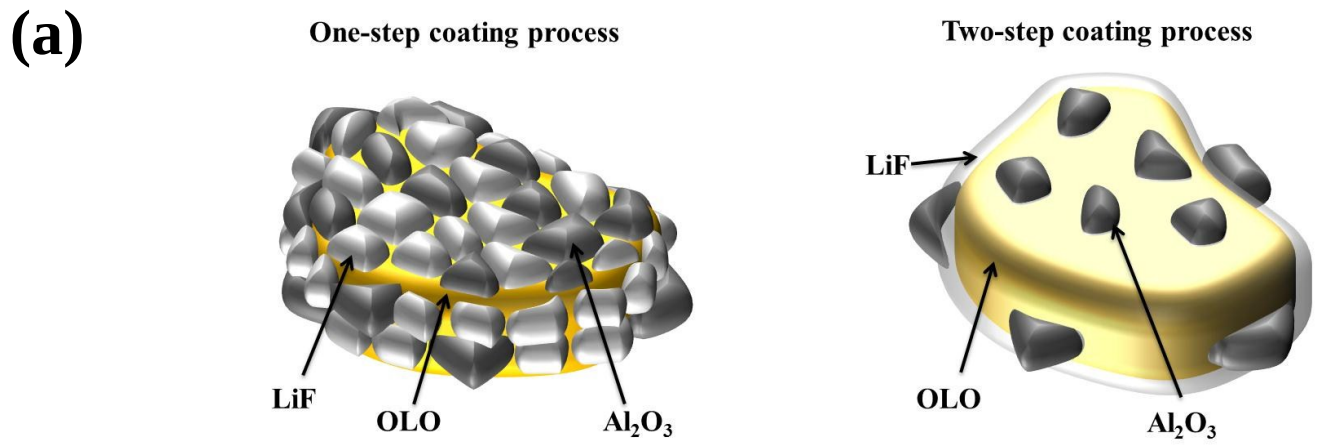

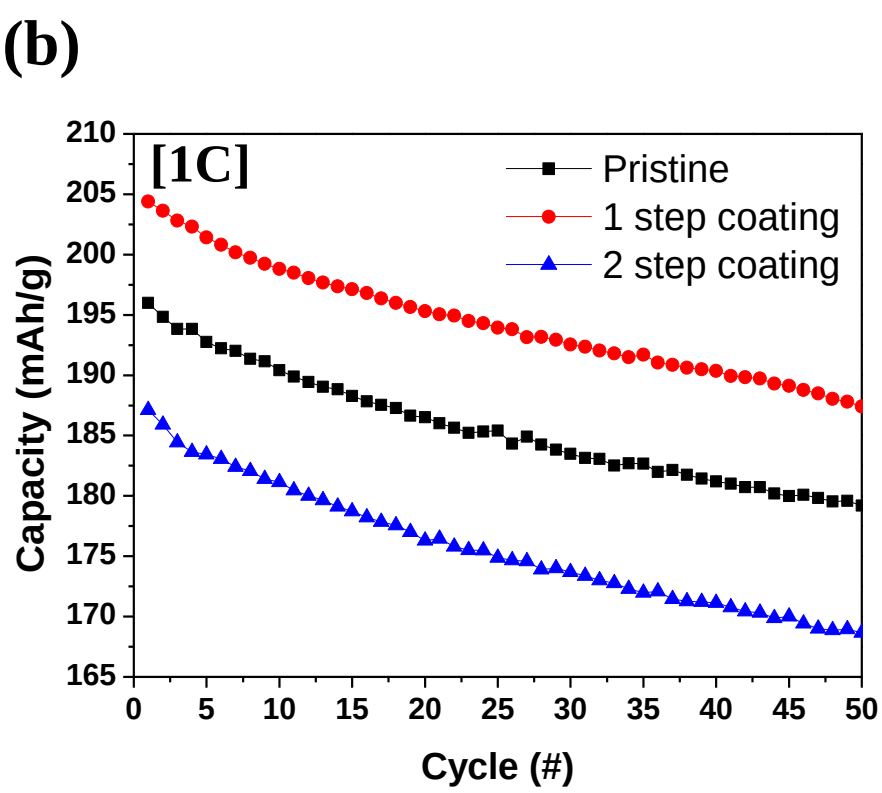

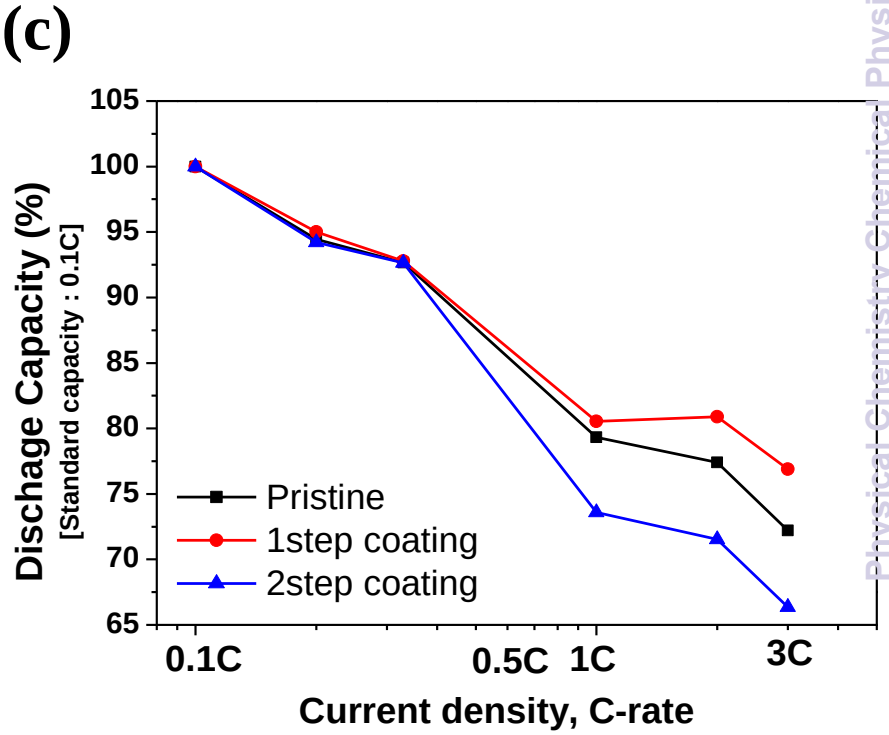

Figure 6